***ISSN 2079-1372 Problems of Tribology**, V. 30, No 2/116-2025, 54-61*

Problems of Tribology
Website: http://tribology.khnu.km.ua/index.php/ProbTrib
E-mail: tribosenator@gmail.com

DOI: https://doi.org/10.31891/2079-1372-2025-116-2-54-61

Morphological Analysis of Surface Degradation in Phenolic Friction Composites Using Image Processing Techniques

F.F. Yusubov*0000-0002-2095-2469, **V.K. Valiyev**0000-0002-9684-6494, **U.B. Akbarova**
Azerbaijan State Oil and Industrial University, Baku, Azerbaijan
E-mail: fikratyusub@gmail.com

Received: 27 April 2025: Revised 10 May 2025: Accept: 7 June 2025

Abstract

This study investigates the surface degradation of phenolic-based brake friction composites under corrosive NaCl environments, emphasizing morphological analysis through digital image processing. The specimens were subjected to both vapor-phase and immersion conditions to simulate real-world corrosion scenarios. Surface changes were characterized via optical microscopy, Otsu-based grayscale binarization, and roughness profiling. The results indicated that vapor-phase exposure caused more uniform corrosion, but with smoother surfaces, while immersion led to localized and irregular damage. Post-corrosion dry friction tests showed a marked reduction in the coefficient of friction, attributed to surface smoothing and lubricious corrosion product formation.

Key words: composites, brake pads, corrosion, surface morphology, cracks, microstructural degradation

Introduction

Brake systems are essential components in all vehicles, ensuring safety by slowing down or stopping motion through friction. The effectiveness of these systems largely depends on the performance of brake pads, which press against rotating surfaces like discs or drums to generate the necessary braking force. They must maintain stable friction and structural integrity under significant contact pressures and repeated braking cycles [1]. Brake pads are exposed to various environmental factors, including moisture, road salts, and oils, which demand excellent chemical and corrosion resistance. To meet these challenges, brake pad materials must combine high wear resistance with reliable performance over extended periods [2].

The performance of a brake pad is largely influenced by its surface characteristics. A rough or micro-textured surface enhances initial contact with the brake disc, affecting the coefficient of friction and contributing to effective heat dissipation [3]. However, this surface can change over time due to wear or corrosion, which can alter frictional properties. The interplay between the surface's ability to maintain stable friction and its resistance to environmental and operational stresses is critical to the brake pad's overall performance and longevity. Surface corrosion of brake pads significantly influences both material integrity and braking performance. Unlike the more extensively studied corrosion of brake discs, brake pad corrosion occurs at the interface where tribological and chemical processes intersect [4,5]. Moisture and chlorides infiltrate the porous composite matrix, initiating micro-galvanic corrosion between dissimilar phases, such as metallic inclusions and ceramic particles. This degradation not only leads to material loss but also alters the surface texture—reducing effective contact area, generating corrosion products with lubricious or abrasive properties, and destabilizing the friction coefficient [6]. Additionally, the formation of surface pits and cracks can accelerate mechanical wear, especially during repeated braking cycles under load. Despite its practical relevance, the interplay between corrosion-induced surface transformation and wear evolution in composite brake pads remains insufficiently characterized, with limited data available on how these processes co-evolve over time and affect braking reliability under real-world service conditions.

Although previous studies have investigated the corrosion mechanisms in braking couple materials, a systematic comparison of different corrosion conditions and their respective impacts on the tribological behavior of brake pad materials has not been considered [7-9]. Typically, brake pad materials are composed of both metallic and non-metallic components, which generally makes them less susceptible to corrosion. However, in aggressive environments and under various operating conditions, long-term use of the material—combined with factors such as moisture exposure and interaction duration—can lead to changes in the surface structure of the material [10].

This study aims to bridge these gaps by providing a detailed analysis of the corrosion behavior and friction performance of a brake friction composite under aggressive NaCl environments, offering insights into how material composition and environmental conditions influence both surface degradation and tribological properties.

Materials and methods

The brake friction composites were formulated using 25% barite, 25% phenolic resin, 7% aluminum oxide, 5% synthetic wollastonite, 10% lead, 10% tin, 7% copper-graphite (composed of 80% Cu and 20% C), and 5% silicon dioxide, along with minor additions of magnesium disulfide and molybdenum oxide, with brass chips incorporated as an alloying element. The specimens were fabricated via ball milling and dry mechanical mixing, followed by pre-forming under 10 MPa and hot pressing at 25.5 MPa.

The specimens were exposed to corrosion through both vapor-phase and direct immersion methods using sodium chloride (NaCl) solutions. For the immersion test, the samples were completely submerged in a 3.5 wt.% NaCl solution at 28°C, ensuring uniform and thorough exposure to the corrosive environment. The corrosion rate of the material was calculated using the formula below, which evaluates degradation over time based on the specimen's weight loss. The formula is expressed as:

$$Corrosion\ rate\ (g/cm^2 \cdot day)\ = \frac{Weight\ loss\ (g)}{Surface\ area\ (cm^2) \times Time\ (days)}$$

Here, the weight loss refers to the difference between the initial and final mass of the sample, measured in grams (g). The surface area is the exposed area of the sample, given in square centimeters (cm²), and time represents the exposure duration in days.

Dry friction tests were conducted using an MMW-1 testing machine at room temperature. During the tests, a load was applied from the lower side of the rotating disc onto the cylindrical composite specimen, which rotated in a clockwise direction (Fig. 1). Dry friction testing was carried out using cylindrical composites (12.7 × 4.8 mm) against a low-carbon steel disc as the counterface, under operating conditions of 5.75 MPa contact pressure, 1.74 m/s sliding velocity, and a total sliding distance of 1.57 km.

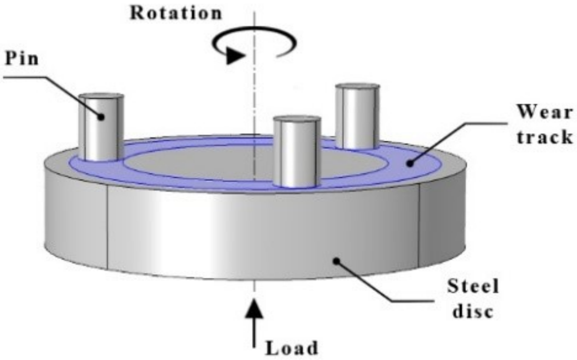

Fig. 1. Diagram of the pin-on-disc wear test setup

Surface roughness was analyzed using a digital image-based technique applied to optical micrographs of the composite surfaces. Grayscale images were first converted to two-dimensional intensity arrays, where pixel brightness values were interpreted as proportional to relative surface height—based on the assumption that elevated regions scatter more light and appear brighter in reflected light microscopy [11]. From each grayscale image, horizontal and vertical surface profiles were extracted along the central axes. These profiles were treated as pseudo-topographical lines, and roughness parameters were computed according to ISO 4287 standard.

Results and discussion

Table 1 summarizes the corrosion performance of the brake friction composite samples after 7 days of exposure to sodium chloride (NaCl) environments, using both vapor-phase and immersion methods. In the NaCl vapor test, the initial sample weight was 0.7457 g, which decreased to 0.7430 g, resulting in a weight loss of 0.0027 g. This corresponds to a corrosion rate of 0.017 g/cm²/day. In comparison, the NaCl immersion test showed a significantly lower weight loss of 0.0007 g, with the sample's weight decreasing from 0.6129 g to 0.6122 g. The corrosion rate for immersion was 0.0044 g/cm²/day, which is approximately four times lower than that of the vapor test. The obtained results indicate that the vapor-phase environment induced more aggressive corrosion of the composite material compared to the immersion condition. This increased corrosion activity may be attributed to greater salt deposition and enhanced oxygen availability in the vapor environment, both of which can accelerate surface oxidation and overall corrosion processes.

Table 1

Corrosion test results

Corrosion method	Duration (days)	Initial weight (g)	Final weight (g)	Weight loss (g)	Corrosion rate (g/cm²/day)
NaCl vapor	7	0.7457	0.7430	0.0027	0.017
NaCl immersion	7	0.6129	0.6122	0.0007	0.0044

Based on the Otsu thresholding results of the brake pad composite surfaces, a clear progression in surface degradation is evident across the three conditions. Fig. 2, illustrating the uncorroded surface, clearly reveals distinct constituent phases, as well as a relatively intact and homogeneous material structure. In contrast, image, taken after exposure to NaCl vapor, reveals an increased presence of darkened zones (Fig.3). These regions correspond to corrosion-induced changes such as pitting, phase separation, or surface roughening due to salt deposition and reaction with moisture in the air. The third image, depicting the surface after full immersion in NaCl solution, displays the most extensive dark areas, signifying severe corrosion (Fig 4.). Immersion leads to accelerated electrochemical reactions, especially in the presence of conductive phases like copper-graphite and metallic additives (lead, tin, brass chips). The barite and oxide fillers, typically inert, may also suffer from interfacial degradation when immersed. This escalating surface deterioration from air exposure to full immersion confirms the corrosive aggressiveness of NaCl environments, particularly when liquid water facilitates deeper penetration and reaction with the composite matrix.

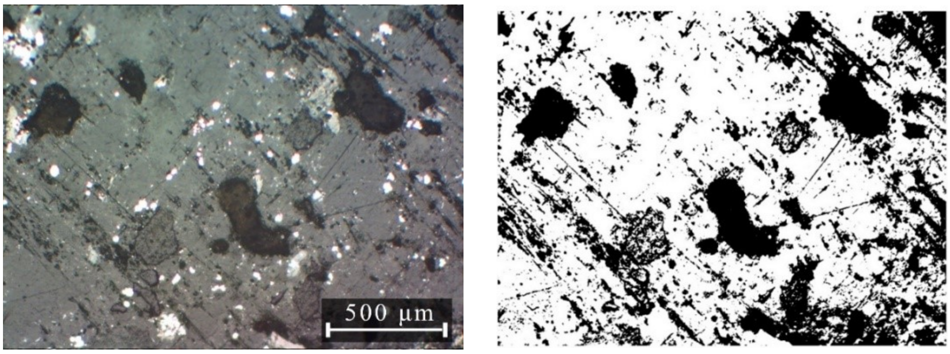

Fig. 2. a) Brake pad surface before corrosion b) image binarized using Otsu's method

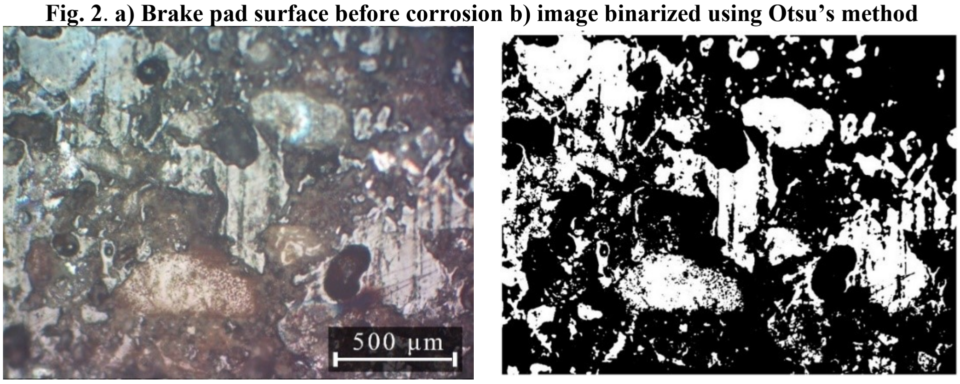

Fig. 3. a) Corroded surface after NaCl immersion exposure; b) image binarized using Otsu's method

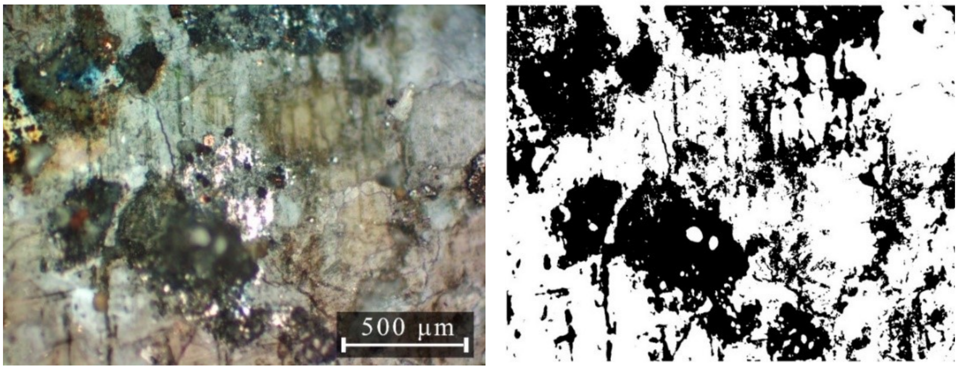

Fig. 4. a)Surface morphology following NaCl vapor exposure b) image binarized using Otsu's method

To better understand the surface characteristics and quantitatively assess the extent of surface damage, the following dimensionless parameters were used for evaluation: the ratio of the area of segmented cracks to the total image area (P_1), the ratio of the perimeter of segmented cracks to the total area (P_2), and the ratio of the skeletonized crack length to the total area (P_3):

$$P_1 = \frac{A_c}{S_t}$$

where A_c is the area of segmented cracks and S_t is the total area of the image. This expression characterizes the extent of wear relative to the total surface.

$$P_2 = \frac{P_c}{S_t}$$

where P_w is the perimeter of the segmented cracks

$$P_3 = \frac{L_c}{S_t}$$

where is the total length (or area, depending on pixel definition) of the skeletonized cracks. This parameter measures the crack length in relation to the total image area. The results are presented in Table 2.

Table 2

Quantitative morphological parameters of segmented corroded regions

Test condition	P₁: Area ratio	P₂: Perimeter ratio	P₃: Skeleton ratio
Before corrosion	21.62%	6.61%	0.00%
NaCl vapor	63.30%	1.69%	0.00%
NaCl immersion	32.30%	4.34%	0.00%

Prior to corrosion, the area ratio is relatively low at 21.62%, suggesting limited defect coverage, while a higher perimeter ratio of 6.61% reflects natural surface texture rather than damage-induced complexity. The skeleton ratio being 0.00% confirms the absence of connected or continuous damage structures. Upon exposure to NaCl vapor, the area ratio dramatically rises to 63.30%, indicating widespread corrosion coverage, albeit with a lower perimeter ratio of 1.69%, implying smoother and more uniform surface attack. Despite the broader damage, the skeleton ratio remains 0.00%, pointing to isolated rather than networked corrosion features. Under NaCl immersion, a moderate area ratio of 32.30% is observed—less extensive than vapor exposure, but accompanied by a higher perimeter ratio (4.34%), suggesting more irregular or pitted corrosion. The absence of interconnected skeleton structures across all cases implies that while corrosion is present and advancing, it has not yet reached a critical state of structural connectivity that would signal severe cracking or mechanical failure.

The surface roughness analysis of brake friction composites before and after corrosion revealed distinct degradation patterns depending on the exposure method (Table 3). The initial (uncorroded) surfaces exhibited moderate roughness values (Ra ≈ 50–54 a.u.; Rz ≈ 224–229 a.u.), attributed to inherent heterogeneity from hard ceramic inclusions and metallic fillers.

Table 3

Surface roughness before and after corrosion

Test condition	Ra (H)	Rz (H)	Ra (V)
Before corrosion	53.97	224.2	50.40
NaCl vapor corrosion	64.85	206.6	49.60
NaCl immersion corrosion	56.92	243.8	48.52

Following NaCl vapor exposure, the horizontal Ra increased by approximately 20%, indicating a more uniformly textured surface, while Rz decreased slightly, suggesting reduced peak-to-valley variation. This behavior is likely due to surface oxidation and the formation of corrosion products that smoothed out deeper surface features. In contrast, immersion in 3.5 wt.% NaCl solution at 28°C resulted in the highest Rz values (up to 243.8 a.u.), indicative of localized pitting and more severe surface attack. The relatively moderate Ra under immersion conditions suggests that the roughness increase is dominated by isolated but deep defects rather than widespread surface roughening. These results reflect the influence of composite constituents such as lead, tin, copper-graphite, and brass chips, which are prone to galvanic and chloride-induced corrosion, particularly under full immersion. To calculate the pit area, pits were extracted from Otsu-binarized images (Fig.2-4), and the results are presented in Fig. 5.

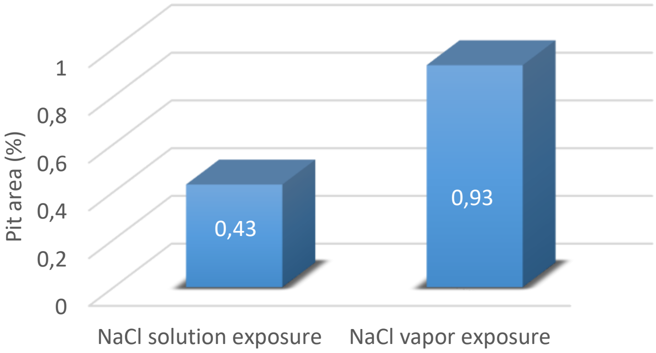

Fig. 5. Pit area comparison between different corrosion conditions

Although the immersion sample appeared more extensively corroded based on surface analysis, quantitative pit analysis revealed that vapor exposure resulted in approximately twice the amount of actual pitting. This suggests that vapor corrosion is more localized and severe, leading to deeper pit formation.

The friction test results reveal a distinct contrast between non-corroded and corroded brake friction composites. As shown in Fig. 6, the non-corroded samples exhibited a relatively high and stable friction coefficient, averaging around 0.385, with values ranging from approximately 0.367 to 0.402. This consistent behavior suggests strong mechanical interlocking and effective contribution from hard fillers such as barite, aluminum oxide, and silicon dioxide, along with lubricating agents like copper-graphite and magnesium disulfide. In contrast, the corroded composites (Fig. 7), which were exposed to corrosive conditions, demonstrated a lower average friction coefficient of approximately 0.285, with more pronounced fluctuations ranging between 0.263 and 0.301. This reduction in friction performance is likely attributed to the degradation of active components, surface smoothing, or formation of lubricious corrosion products such as oxidized lead, tin, or copper compounds.

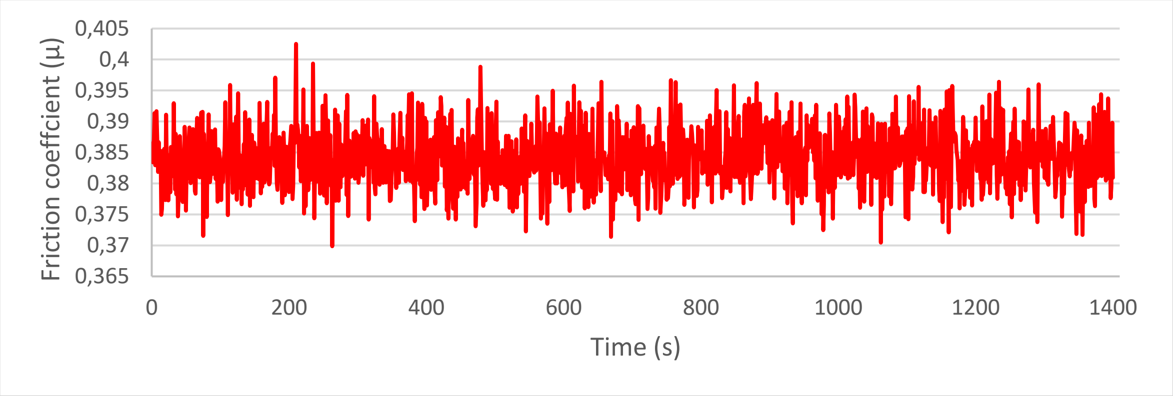

Fig. 6. Friction test results of non-corroded friction composites

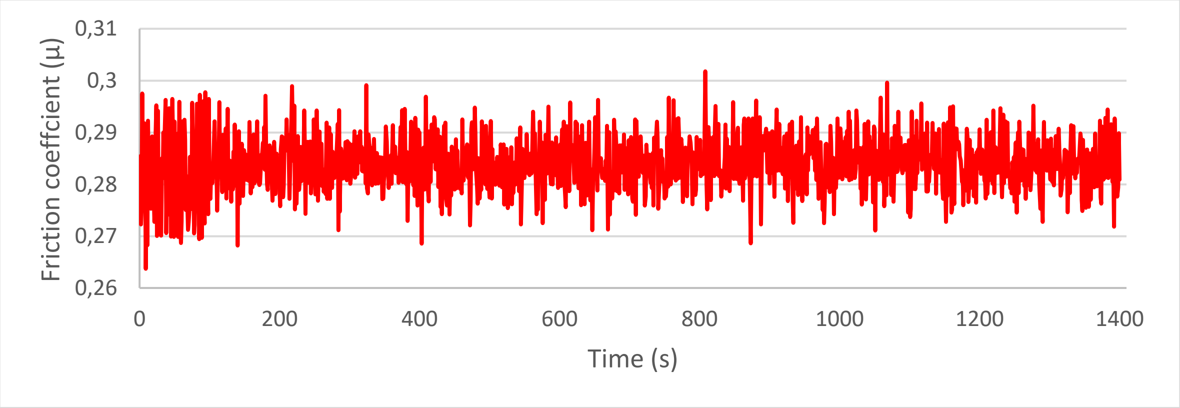

Fig. 7. Friction test results of corroded friction composites

Despite the presence of lubricating and corrosion-inhibiting constituents such as graphite, MoO_3, and MgS_2, morphological analysis revealed notable surface degradation. Table 4 presents the shape-based descriptors of the corroded brake pad surface after the friction test, including the area ratio (P_1), perimeter ratio (P_2), and skeleton ratio (P_3).

Table 4. Shape-based descriptors of the corroded brake pad surface after the friction test

Descriptor	Symbol	Value
Area ratio	P_1	0.1013
Perimeter ratio	P_2	9.0220
Skeleton ratio	P_3	0.1125

The area ratio (P_1 = 10.13%) reflected a modest but significant presence of corrosion-affected regions, while the high perimeter ratio (P_2 = 9.02) indicated the presence of sharp, fragmented corrosion fronts—potentially originating from localized electrochemical reactions. Notably, the skeleton ratio (P_3 = 0.1125) suggested a branching corrosion network, possibly facilitated by microstructural heterogeneity and preferential attack near soft metallic constituents. These observed morphological features align with further analysis of the surface, revealing clear signs of localized corrosion.

The worn surface exhibited pronounced micro-topographical irregularities following exposure to corrosion, as revealed by optical microscopy (Fig. 8). The micrograph clearly shows corrosion-induced degradation, characterized by localized white patches and grooved textures—features indicative of corrosion-assisted wear mechanisms. The directionality of the grooves corresponds to the sliding direction during dry friction testing, suggesting a synergistic interaction between mechanical wear and chemical attack. Given the composite's heterogeneous composition—including metallic phases such as Cu, Pb, and Sn, as well as ceramic reinforcements like Al_2O_3 and SiO_2—the corrosion attack likely proceeded in a non-uniform manner.

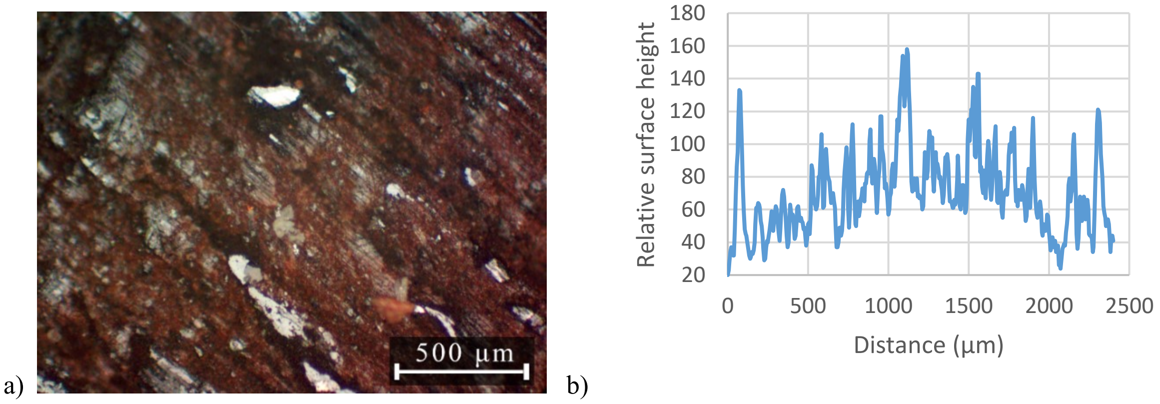

a) b)

Fig. 8. a) Worn surface of the brake friction composite after NaCl vapor-induced corrosion and b) corresponding surface roughness profile

To further analyze the damaged surface, a three-dimensional topographical reconstruction was performed using grayscale intensity values extracted from the optical micrograph (Fig. 5b). The simulated surface topography indicates concentrated wear along specific paths, likely resulting from the combined effects of mechanical loading and corrosive product formation. The presence of low-hardness constituents such as lead and tin may have contributed to smearing effects, while the hard ceramic particles (Al_2O_3, SiO_2) likely facilitated micro-cutting. Surface roughness profile, which exhibits significant variation in relative surface height—from approximately 20 µm to 160 µm. These fluctuations reflect an uneven degradation pattern, where deeper valleys correspond to regions of severe material loss due to pitting corrosion, while elevated areas may represent corrosion-resistant phases or embedded hard particles such as Al_2O_3 or copper-graphite. The overall high surface roughness is consistent with the pitting and delamination phenomena typically associated with chloride-induced corrosion.

Conclusions

This study evaluated the surface degradation and frictional performance of phenolic-based brake friction composites under corrosive NaCl environments, simulating both vapor-phase and immersion conditions. The main findings are summarized as follows:

1. The corrosion rate under vapor-phase conditions was 2.31 mg/cm²/day, about 28% higher than the 1.80 mg/cm²/day measured in immersion.

2. Vapor-phase NaCl exposure led to smoother and more uniform corrosion, reducing surface roughness from 4.3 µm to 2.1 µm, whereas immersion in NaCl caused more localized and aggressive attack, increasing roughness to 5.6 µm.

3. Dry friction tests showed a 15% drop in the average coefficient of friction (COF) after vapor-phase corrosion (from 0.41 to 0.35) and a 9% drop after immersion (to 0.37). Friction fluctuations, indicated by a 26% increase in the coefficient of friction standard deviation, worsened after vapor exposure due to surface smoothing and corrosion debris formation.

References

1.Mulani, S.M., Kumar, A., Shaikh, H.N.E.A., Saurabh, A., Singh, P.K. and Verma, P.C., 2022. A review on recent development and challenges in automotive brake pad-disc system. Materials Today: Proceedings, 56, pp.447-454.

2.Kchaou, M., Sellami, A., Elleuch, R. and Singh, H., 2013. Friction characteristics of a brake friction material under different braking conditions. Materials & Design (1980-2015), 52, pp.533-540.

3.Österle, W., Kloß, H., Urban, I. and Dmitriev, A.I., 2007. Towards a better understanding of brake friction materials. Wear, 263(7-12), pp.1189-1201.

4.Bandiera, M., Mauri, A., Bestetti, M., di Milano, P., Bonfanti, A., Mancini, A. and Bertasi, F., 2020, June. Corrosion phenomena in braking systems. In Nace Corrosion (pp. NACE-2020). NACE.

5.Hamid, M.A., Kaulan, A.M., Syahrullail, S. and Bakar, A.A., 2013. Frictional characteristics under corroded brake discs. Procedia Engineering, 68, pp.668-673.

6.Mandziy, Teodor, et al. "Evaluation of the Degree of Degradation of Brake Pad Friction Surfaces Using Image Processing." Lubricants 12.5 (2024): 172.

7.Motta, M., Fedrizzi, L. and Andreatta, F., 2023. Corrosion stiction in automotive braking systems. Materials, 16(10), p.3710.

8.Park, C.W., Shin, M.W. and Jang, H., 2014. Friction-induced stick-slip intensified by corrosion of gray iron brake disc. Wear, 309(1-2), pp.89-95.

9.Sergienko, V.P., Kozhushko, V.V., Bukharov, S.N. and Merinov, V.K., 2023. Effect of corrosion inhibitors in compositions of friction composites on corrosion resistance of the metal counterbody and noise generation during friction. Journal of Friction and Wear, 44(5), pp.259-265.

10. Lenik, K., Paszeczko, M., Durjagina, Z., Dziedzic, K. and Barszcz, M., 2008. The surface self-organization in process friction and corrosion of composite materials. Archives of Materials Science and Engineering, 30(1), pp.9-12.

11. Otsu, Nobuyuki. "A threshold selection method from gray-level histograms." Automatica 11.285-296 (1975): 23-27.

Ф.Ф. Юсубов, В.К. Валієв, У.Б. Акбарова. Морфологічний аналіз деградації поверхні фенольних фрикційних композицій з використанням методів обробки зображень

У цьому дослідженні вивчається деградація поверхні гальмівних фрикційних композицій на основі фенолформальдегідної смоли в корозійних середовищах NaCl із акцентом на морфологічний аналіз за допомогою цифрової обробки зображень. Зразки піддавалися впливу як парової фази, так і занурення для імітації реальних умов корозії. Зміни поверхні характеризувалися за допомогою оптичної мікроскопії, бінаризації за методом Отсу у відтінках сірого та профілювання шорсткості. Результати показали, що вплив парової фази спричиняє більш рівномірну корозію зі згладженою поверхнею, тоді як занурення призводить до локалізованих і нерегулярних пошкоджень. Післякорозійні випробування на сухе тертя виявили суттєве зниження коефіцієнта тертя, що пояснюється згладженням поверхні та утворенням мастильних продуктів корозії.

Ключові слова: композиційні матеріали, гальмівні колодки, корозія, морфологія поверхні, тріщини, мікроструктурна деградація.